

Approved For Release STAT
2009/08/17 :
CIA-RDP88-00904R000100100

Dec

Approved For Release
2009/08/17 :
CIA-RDP88-00904R000100100



Third United Nations
International Conference
on the Peaceful Uses
of Atomic Energy

A/CONF.28/P/346

USSR

May 1964

Original: RUSSIAN

Confidential until official release during Conference

EXTRACTION PROCESSES AND THEIR MATHEMATICAL DESCRIPTION

Rozen A.M., Bezzubova A.I., Elatontsev B.V., Khorkhorina L.P.,
Nemirovsky A.M., Nikolotova Z.I., Phushlenkov M.F., Reshetko Yu.V.
Shuvalov O.N., Teterin E.G., Vasiliev V.A., Yurkin V.G.

In the present paper which generalizes and develops papers¹⁻¹⁵) the quantitative regularities of the extraction chemistry and engineering are studied and interpreted.

1.Extraction Equilibria

1.General. The extraction equilibrium regularities are discussed using the extraction of uranyl and other actinide nitrates by neutral organophosphoric compounds (for general discussion see⁴) as an example. These systems show the electrolyte-nonelectrolyte equilibrium when the chemical bond of an extractant with a compound being recovered is necessary to overcome the electrostatic interaction in an aqueous phase. However, the bond should be sufficiently weak to permit stripping (the interaction energy $< 10 \frac{\text{kcal}}{\text{mole}}$). Accordingly, to interpret the extraction power of solvents the theory of chemical bond is required while due to the chemical interaction weakness when describing the dependence of equilibria on the extraction conditions it is necessary to consider the contribution of the Van-der-Waals (up to 3kcal/mole) and especially electrostatic interactions to the chemical potential in terms of the solution theory (the electrolyte solution theory for the aqueous phase processes while the multi-component nonelectrolyte one for the organic phase).

The extraction, not complicated by the hydrolysis or formation of anionic complexes is described by: $\text{Me}^{n+} + n\text{A}^- + q\text{S} + h\text{H}_2\text{O} = \text{MeA}_n\text{qS} \cdot h\text{H}_2\text{O}$ where A is an anion, S, an extractant. Accordingly, the distribution coefficient for unhydrated solvates ($\text{A} = \text{NO}_3$) will be:

$$\alpha = y/x = K(\text{NO}_3)^n \dot{\gamma}_{\pm}^{n+1} (\text{S})^q \dot{\gamma}_{\text{S}}^q / \dot{\gamma}_{\text{C}} \quad (1.1)$$

where K is a thermodynamic distribution constant; y and x, concentrations of a compound in aqueous (a.p.) and organic (o.p.) phases, the round brackets denote concentrations, ($\dot{\gamma}_{\pm}, \dot{\gamma}_{\text{C}}, \dot{\gamma}_{\text{S}}$ are activity coefficients of ions in a.p., of a solvate in o.p. and of an extractant, the dot

25 YEAR RE-REVIEW

notes the concentration coefficients: $\gamma=1$ at $x=0$ or $y=0$; $\gamma_s=1$ at $N_s=1$

The terms of the equation define: K —an extractability; $(NO_3)^{n,n+1}$ processes in a.p., salting out; S^q —the effect of dilution due to solvation (in case of the extraction of several compounds it describes the competition for a free extractant); $\gamma_s^q/\gamma_c^q = dil$, is the effect of the diluent peculiarity (weak interactions in o.p.). These effects are to be discussed consecutively.

Extractability depends on the extraction power of the solvent and the forces retaining a compound in a.p. According to ^{4),5)}

$$K_N = \exp(\mu_{aq}^0 - \mu_{org}^0) / RT = \gamma_+^{n+1}(0)_{aq} / \gamma(0)_{org} \approx \gamma_+^{n+1}(0)_{aq} (1 + K_S) \quad (1.1)$$

where $\gamma(0)$ is the γ value at a zero concentration, K_S , the solvation constant in o.p. The values of $\gamma(0)$ so far determined only for HCl and HNO₃ are very low ($\gamma^2 = 3 \cdot 10^{-5}$ and $2.1 \cdot 10^{-2}$, respectively) i.e. ions are strongly bonded with water^{x)}. Therefore for the effective extraction a strong solvation is needed in o.p.

Extraction power of phosphine oxides is maximum and diminishes on substitution of alkyl groups R by electrophilic ones (Ro, Ph, Cl)^{16,17}. To obtain the quantitative regularities it is necessary to improve the criteria of extractability and structure. The effective constant $\bar{K} = K \gamma_s^q / \gamma_c^q = K dil^{xx}$ and the electronegativity (EN) of groups, X, were assumed to be such criteria⁶⁾. To improve the EN scale¹⁸⁾ the infrared spectra of a number of organophosphoric compounds R₁R₂R₃PO were investigated and the following scales were obtained (fig. 2a, b):

$$a) X_F = 4.0; \sum X = X_{RI} + X_{R2} + X_{R3} = 6 + 0.024(\omega_{PO} - 1170) \quad (1.2)$$

$$b) X_F = 3.9; \sum X = 6.6 + 0.021(\omega_{PO} - 1170) \quad (1.3)$$

| Group | R | OR | Ph | OPh | CH ₂ Cl | CCl ₃ | Ph | OPh | CH ₂ Cl | CH ₂ ClCH ₂ | CCl ₃ | |
|----------------------|-------------|------|-----|-----|--------------------|------------------|--------------------------|------|--------------------|-----------------------------------|------------------|-----|
| Scale B _U | X, Spectral | | | | | | X eff. (from extraction) | | | | | |
| 18) | 1.65 | 2.0 | 3.0 | 2.4 | 3.2 | 2.85 | 3.35 | 2.7 | 3.5 | 3.3 | 2.7 | 4.6 |
| 1.2 | 1.85 | 2.0 | 2.9 | 2.3 | 3.1 | 2.6 | 3.2 | 2.65 | 3.4 | 3.1 | 2.6 | 4.3 |
| 1.3 | 2.2 | 2.25 | 3.0 | 2.5 | 3.17 | 2.8 | 3.3 | 2.8 | 3.47 | 3.2 | 2.8 | 4.2 |

Lg K (the free energy) drops approximately linearly with the increase of EN, the number of radicals, n_{OR} and ω_{PO} when alkyl radicals are substituted by ethereal ones (fig. 1), (i.e. when the negative O-charge diminishes):

$$\lg K = A - B \sum X = A_1 - B_1 n_{OR} = A_2 - B_2 \omega_{PO} \quad (1.4)$$

x) Particularly for HCl, due to which it is more poorly extracted by TBP ($K_{HCl} \approx 2 \cdot 10^{-4}$, $K_{HNO_3} \approx 0.2$), though the bond strength of both the acids with TBP is close. $K_S, HCl \approx 7$, $K_S, HNO_3 \approx 10$.

xx) The experiments were carried out using CCl₄ for which $dil \approx 1$. The U, Pu extraction isotherms were measured for the K calculation reliability, ΔH was determined from the lgK temperature dependence.

where constants A and B depend on the nature of the compounds extracted. A stronger extractability decrease when introducing phenyl or chlormethyl radicals is approximately described (fig. 1b)^x by eq (1.4). with the help of effective (increased) EN, $X_{ef} = X_a + \Delta X_{ef} = X_a + \mu \Delta X$; where X_a is EN of the alkyl radical substituted, $\Delta X = X - X_a$, $\mu = \text{const} \approx 2$ (e.g. $X_{CCl_3} - X_a = 1,35$; $X_{CCl_3}^{ef} - X_a = 2,6$, $\mu \approx 1,9$).

The influence of the entropy or steric factors is one of the reasons effecting a difference between X_{ef} and X as EN is responsible only for the change of the binding energy but not for all the free energy. In fact, the deviation from the general regularity is less for ΔH as compared to ΔF (fig. 2c, d), i.e. $-\Delta H = A_3 - B_3 \sum X = A_4 - B_4 \sum \omega_{PO}$.

With the hydrocarbon chain elongation n_c , EN is slightly decreased only for the first members of the series while the steric difficulties are increased, which results in the weak maximum of K observed at $n_c = 6-7$ (fig. 1d, $\bar{n}_c \approx \sum n_c / 3$). To describe the effect of n_c i.e. the influence of the entropy-steric factors, the dependence $\lg K = p + q(C/O)^{20}$, determined for ethers, can be used as the EN change cannot explain the constant decrease and $C/O = 2n_c$. As for the highly branched radicals the effective hydrocarbon chain length may be $l > n_c$, the general equation of the extraction power is

$$-\Delta F^0/RT = \lg K = A - B \sum X_{ef} - q_l = A_3 - B_3 \sum X - q_l' \quad (1.5)$$

The similar dependencies are expected in extracting by amines and acidic extractants (in this case $B < 0$); X_{ef} differing from X even more owing to polymerization⁶).

Salting out Theory⁴, based on the electrolyte solution theory, allows the effect of the salting out agent to be predicted, when the effective diameter of the extracted ions, the hydration numbers of ions and of the salting out agent are known. When computing it is convenient to express the activity coefficients by Harned's equation, and in case of a linear concentration dependence of γ by Rozen's one,

$$\lg \gamma(x_{me}, x_{salt.}) = \lg \gamma(x_{me}, 0) + (\delta^* - \delta) I_{salt.} \quad (1.5)$$

For UO_2^{2+} and PuO_2^{2+} nitrates $\lg \gamma(x_{me}, 0) = -0,46 + 0,116 I$, i.e. $\delta_{UO_2^{2+}}^* = \delta_{PuO_2^{2+}}^* = 0,116$

The approximate values of Harned's coefficients are:

| Cation | H ⁺ | Na ⁺ | NH ₄ ⁺ | Mg ⁺⁺ , Be ⁺⁺ , Ca ⁺⁺ | Al ⁺⁺⁺ |
|------------|----------------|-----------------|------------------------------|--|-------------------|
| for U(VI) | 0 | +0.06 | 0.08 | 0.033 | 0.054 |
| for Pu(VI) | 0 | - | 0.13 | 0.053 | 0.078 |

x) Fig. 1a, b, c: I-(RO)₂PO, II(RO)₂R PO, III ROR₂PO, IV R₃PO (C₈, oC₄); fig. 1b: 1-(RO)₂PhO PO; 2(CH₂ClCH₂O)₃PO, 3-(RO)₂PhPO, 4-(RO)₂CCl₃PO (Ph-phenyl); fig. 2: DHPPhP-dihexylphenylphosphonate, DHCLMP-dihexylchlormethylphosphonate.

Effect of Diluents. The solvate formation results in the extraction dependence on the extractant concentration $S(\alpha \sim S^q)$ which is not affected by the diluent nature; the latter determining the value of the diluent parameter $dil = \gamma_s^2 / \gamma_c$. The activity coefficients in multicomponent systems taking part in dil may be expressed and interpreted by the properties of binary systems with the help of the solution theory. The activity coefficients in binary systems diluent-TBP and diluent-uranyl nitrate solvate, are approximately described by the equation with two constants: $\lg \gamma_1 = \varphi_2^2 (b_{12} - 2\varphi_1 \Delta_{12})$, $\Delta_{12} = b_{12} - b_{21} V_2 / V_1$, while the data on the three-component systems by the equation with data on the binary systems^{xxx} at $C=0$. Acid and water taken into account the expression dil becomes most complicated and contains 20 constants, describing all the possible binary interactions; accordingly dil depends on the nature of the diluent and the compound being extracted (fig. 3a, b) as well as on the acid concentration (fig. 3c)^{xx}. The dil values derived from the data on the activity coefficients of binary systems and from the extraction data are in agreement^{xxx}. The dil values are similar for all the diluents except CHCl_3 , although the non-ideality sign in the TBP-diluent solution is different and γ_T^2 varies by 100 times. It is explained by the similarity of the properties of TBP and solvate (with the higher non-ideality in solvate systems) due to which the interactions TBP-diluent and solvate-diluent affecting dil in an opposite way are partially compensated, $b_{31} \approx 2b_{21}$. As compared to CCl_4 , dil is increased (fig. 3a) due to the predominance of the interaction with TBP (hexane) or with solvate (C_6H_6). The positive non-ideality of the TBP and solvate solutions in saturated hydrocarbons shows that the interaction between similar molecules is stronger than that between different ones, which is typical of the Van-der-Waals forces. The strong negative non-ideality $\lg \gamma_1 = (1-\varphi_1) [\varphi_2 (b_{12} - 2b_{21} \Delta_{12}) + \varphi_3 (b_{13} - 2\varphi_1 \Delta_{13})] + \varphi_2 \varphi_3 [(\Delta_{12} - C)(1-2\varphi_1) - b_{23} V_2 / V_1]$; C , is ternary constant, nos of components: 1-diluent, 2, extractant, 3, solvate, φ , the volume fraction; V , the molal volume.

xx) For the extraction of metal microamounts ($y_3 \sim C$) with diluted extractant ($y_2 \sim 0$) one obtains simple eqns, the form of which depends on the selected standard state of the solvate: dil^I - a pure solvate, II - a diluted solution in dry TBP, III - a solution in TBP, containing water and acid. E.g. $\lg dil^I = 2b_{21} - b_{31}$, $\lg dil^{II} = 2b_{21} - b_{31} + b_{32}$, i.e. the deviation from ideality is due to the extractant-diluent (b_{21}), solvate-diluent (b_{31}) and solvate-extractant (b_{32}) interactions.

xxx) For C_6H_{14} , C_6H_6 and CHCl_3 from extraction $dil^I / dil^I_{\text{CCl}_4} = \bar{K} / \bar{K}_{\text{CCl}_4} = 1.55$; 2.35; 0.02, from γ_1^2 : 1.55; 2.42; 0.013. ($dil^I_{\text{CCl}_4} = \gamma_2^2(0) / \gamma_3(0) \approx 1$). Nos of curves in fig. 4a, b, d: 1, 5 CCl_4 diluent; 2, 6 C_6H_6 ; 3, 7 hexane; 4, 8 CHCl_3 .

746

ity in the TBP-CHCl₃ system results from the hydrogen bond formation as evidenced by the spectroscopic data^{21,14)} and the high value of the heat of mixing (fig.4d). The main reason for the moderate negative non-ideality in systems with CCl₄ and C₆H₆ (and in CHCl₃-solvate) is an athermal effect, i.e. the solution entropy increase due to the difference in sizes of the component molecules (fig.4a,b). However, the negative non-ideality is not confined to the athermal effect as the enthalpy of mixing is negative. Thus, in these systems the "molecular" negative non-ideality ($\gamma = \gamma/\gamma^{\text{atherm.}} < 1$) exists^{x)} which may be interpreted by the unstable compound formation⁵⁾. The uranyl nitrate solvate-TBP system is also characterized by the negative non-ideality ($b_{23} \approx -0.6$) and a high value of the heat of mixing ($h_{0.5}^E = -775 \frac{\text{cal}}{\text{mole}}$) which may be interpreted by trisolvate $\text{UO}_2(\text{NO}_3)_2 \cdot 3\text{TBP}$ formation with $K_s = 1-2$. The interaction of diluents with solvates of Th and Pu(IV) nitrates is similar to that with uranyl nitrate solvate; but for Th solvate, the positive non-ideality is stronger in the systems with saturated hydrocarbons which results in the formation of two organic phases. The solutions of Th solvate in CCl₄ and in C₆H₆ are close to athermal ones ($h_{0.5}^E \approx 50 \text{ cal/mole}$) i.e. there is even a small molecular positive non-ideality. When substituting ethereal groups by alkyl ones (TBP-TOPO series) the activity coefficients of CCl₄, C₂H₄Cl₂ and CHCl₃ and, hence, the extractant-diluent interactions are markedly changed only for TBPO¹⁵⁾ (fig.4c).

The Extraction Isotherm Calculation. In case of the concurrent distribution of U, Pu and HNO₃ macroamounts one obtains⁸⁾:

$$y_U = f_U S^2; \quad y_{\text{Pu}} = f_{\text{Pu}} S^2; \quad y_H = (f_{1H} + 2f_{2H}) S \quad (1.6)^{xx)}$$

$$S = 2S_0 / (1 + f_{1H} + f_{2H} (1 + \sqrt{1 + 8f_{2H} S_0})); \quad \bar{S}_0 = S_0 / (1 + \beta_U / 2) \quad (1.7)$$

where y and x are concn. of compounds in organic and aqueous phases, S and S_0 are free and initial extractant concentrations

$$f_U = \tilde{k}_U x_U \text{NO}_3^2, \quad f_{\text{Pu}} = \tilde{k}_{\text{Pu}} x_{\text{Pu}} \text{NO}_3^4, \quad f_{1H} = \tilde{k}_{1H} x_H \text{NO}_3, \quad f_{2H} = \tilde{k}_{2H} x_H^2 \text{NO}_3^2$$

$$\text{NO}_3 = x_H + 2x_U + 4x_{\text{Pu}} + z_1 x_{\text{salt},1}; \quad \beta_U = 0.00247 S_0 / (0.747 + 0.232 S_0), \quad \beta_H = \beta_U / 2.$$

For TBP $\tilde{k}_U = \tilde{K}_U \gamma_1 \approx 7.1 \cdot 10^{0.564} (x_U + x_H / 3 + x_{\text{Pu}})$, $k_{1H} = 0.19$, $k_{2H} = 0.0004$. If the component concentrations are related to the solvent volumes, then $\beta_H = \beta_U = 0$; $\tilde{k}_U = 5.95 \cdot 10^{0.625} (x_U + x_H / 3 + x_{\text{Pu}})$; $k_{1H} = 0.174$; $k_{2H} = 0.0002$.

x) Probably, there is a weak acceptor-donor interaction between π -electrons of benzene and uncompleted Cl 3d-orbitals with TBP.
xx) Eqns. (1.6) are obtained by the combined solution of U, Pu and HNO₃ distribution eqns (1.1).

Extraction Cascades

Calculation of Cascades. If the apparatuses are not numerous it is convenient to calculate graphically (fig. 5a) the macrocomponent distribution over the extractor stages by the method of successive approximations⁹⁾. The distribution of elements present in micro-amounts is calculated analytically, fig. 6. The equations are obtained by the combined solution of equations of equilibrium $y_i = \alpha_i x_i$ and material balance which for some i-stage is:

$$L_{i-1}x_{i-1} + V_{i+1}y_{i+1} = L_i x_i + V_i y_i, \quad (2.1)$$

where L and V are volumes of a.p. and o.p. The decontamination factor K_d , in the extraction section at $\alpha_1 n \ll 1$ determined by the extraction conditions at the first stage does not depend on the cascade (column) length. Conversely, in the scrubbing section at $\alpha' n \ll 1$, K_d depends on the number of the stages; if $\alpha' = \text{const.}$

$$K_d, \text{casc.} \approx (1/\alpha_1 n_1) \cdot 1/(\alpha' n')^{N'}$$

If $\alpha' n' > 1$, the scrubbing is not effective:

$$K_d, \text{scrub.} \approx 1 + 1/(\alpha' n') + 1/(\alpha_1' n')(\alpha_2' n') + \dots \leq 2 \quad (2.2)$$

e.g. for Ru at $\alpha' = 0.2$ and $n' = 10$ we obtain $K_{\text{scrub.}} \approx 2$. If the extraction is accompanied by a chemical reaction (the reduction stripping), the element concentration in the solution at the i-stage which would be $x_i^0 = x_{i-1} + n(y_{i+1} - y_i)$ in the absence of the reaction, will be $x_i = x_i^0 e^{-k_i t_i}$, k_i , the rate constant^{x)}; t_i the time of the contact. Assuming $y_i = \alpha_i x_i$, we obtain the equation describing the process in the cascade:

$$x_i(\alpha_i + e^{k_i t_i}) = x_{i-1} + n y_{i+1} = x_{i-1} + \bar{\alpha}_{i+1} x_{i+1} \quad (2.4)$$

If the reduction is effective ($e^{k_i t_i} > 10$) so that the Pu(IV) concentration in a.p. at the i-stage inlet $x_{i-1} \approx 0$, a simple relationship between the concentration of the elements not reduced and the initial one (y_{N+1}) is obtained

$$y_1 = y_{N+1} / \lambda_1 \lambda_2 \dots \lambda_N; \quad y_i = y_{N+1} / \lambda_{i+1} \lambda_{i+2} \dots \lambda_N, \quad (2.5)$$

where $\lambda_i = 1 + e^{k_i t_i} / \bar{\alpha}_i$, effective stage reduction coefficient.

The above calculation method based on the stagewise contact pattern describes the process in the column satisfactorily (fig. 5c). If two

x) The values of the rate constants may be estimated from data²²⁾. $k = 2000 [\text{Fe}][\text{Pu}^{4+}]$, provided that $\text{Pu}^{4+} = \text{Pu}(\text{IV}) / (1 + \sum \beta_j \text{NO}_3^j) = \text{Pu}(\text{IV}) / (1 + S)$, where β_j is constant of complexing with nitrate ions. It is interesting to note that too low rate constants are obtained when using β found by the extraction method^{3c)}: at $\text{Fe} = 0.04 \text{ m/l}$ and $x_H = 2 \text{ m/l}$, $S = 360$, $1/k_{\text{calc.}} = 4 \text{ min.}$ while $1/k_{\text{exp.}} < 10 \text{ sec.}$ The extraction method overestimates the β -values.

actinide elements present in macroamounts and when a great number of calculations are needed (the static characteristic determination) EC should be used. We employed the programmes of direct (Ural I) and stagewise (Minsk I) computing. In the latter case the equations of equilibrium (1.7), of material balance (2.1) and those of mixing are used. The programme provides for the minimization of the deviation of the calculated inlet concentrations from the fixed ones by affecting the assumed values of the waste concentrations x_N . Direct computing lies in the combined solution of equations relating the material concentrations to the value at all the cascade stages¹⁵⁾. The microcomponent concentrations are computed after the actinide and acid determinations using an additional programme.

Static characteristics of the extractor processes are determined by a number of variables ($L_0, L', V_0, x_U^0, x_H^0, S$, etc.), their influence may be approximately described as an action of one generalized parameter η , the degree of approximation to the limiting conditions (the flow theoretically minimum one ratio)¹⁰⁾

$$\eta = y/y_p = V_{\min}/V = 1/(\alpha n)_1, \quad (2.6)$$

(where y, y_p are maximum operating and equilibrium U-concentrations in o.p., V and V_{\min} are operating and minimum o.p. flows). It is seen from the illustrative calculation of the Purex extraction-scrubbing column (the impurity effect on the Zr and Pu microamounts was neglected) ($N=4; N'=1, L=76, 5, L'=56, 2, V=383, x_U^0=1.8m/l, x_H^0=0.95m/l, (x_H^0)'=2m/l, T_0=1.2m/l$). The data on U^{238} , HNO_3^{7a} , Pu^{239} , Zr^{90} and Ru^{23} were used¹⁰⁾. The decontamination from Ru was estimated by the separate distribution of tri- and dinitroso-nitrates RuT and RuD ($\alpha_{Ru} = C_T \alpha_T + C_D \alpha_D$) where C is a fraction of species in a.p. Data²³⁾ were recalculated for U-solutions (fig. 7g); it was assumed that $C_T^0 = f(x_H^0) = 0.025$, and in the scrubbing section $C_T = 1, \alpha_{Ru} = \alpha_T$. The flows L^0, V and concentrations x_U^0, T were varied. As it follows from figs. 7, 8 with the η growth the uranium zone is expanded, the accumulation of Pu and Ru increases (the accumulation decrease at $\eta > 99\%$ results from the species losses due to the insufficient stage number), the waste concentrations of U and Pu and K_d from Zr and Ru^{23} rise. Fig. 8 also shows that the static characteristics of the extractor are defined by the approximation degree to the limiting conditions while the way of approximation $x) As \alpha_{Ru} > \alpha_{Pu}$, RuT is extracted completely and $K_{Ru} = 1/C_T^0 \approx 50$ does not depend on η ; however the RuT accumulation is very large (fig. 7e) and if the reaction $RuT-RuD$ in the presence of U is rapid enough, K_{Ru} increases with η . 346

is of little importance. This conclusion is also true of the extraction stage number change.

Optimization of Conditions. A possible way of optimization is a maintenance of the maximum K_d (high η) at the permissible U, Pu losses. Introduction of the optimization criterion is an alternative method. Assuming the conditions providing for the maximum K_d with the minimum loss of U and Pu and minimum Pu accumulation to be optimum, a criterion is

$$\text{Opt.} = K_{\text{Zr}}^m K_{\text{Pu}}^n / (X_N^{\text{Pu}})^r (q_{\text{Pu}})^s \quad (2.7)$$

where m, n, r and s are coefficients characterizing the significance of each factor when processing various fuels^{x)}. In many cases all these factors are equal, $m=n=r=s=1$ (fig. 9d, curve 1). When processing natural U the Pu accumulation is of no importance, $s=0$ (curve 2). If the highly active material is processed the importance of the decontamination increases and $m=n=2$ may be assumed (curve 3). The range of the optimum conditions is $\eta=0.90-0.99$; the greater is the importance attached to the decontamination, the higher is η_{opt} . The use of conditions close to limiting ones is possible only with a sensitive systems of control (e.g. with that retaining the uranium front location in the extractor).

Extraction Dynamics. If $dy/dx = \alpha = \text{const}$, the nonstationary mass-transfer eq.^{xx)} may be solved either approximately by the similarity method^{13,24)} or exactly by the operational one²⁴⁾. At $t > t_0$

$$x_0 - x(z, t) \approx (x_0 - x_p)(1 - e^{-t/t_0}), \quad (2.8)$$

where $x_p(z) = x(z, \infty)$ is the equilibrium concentration, while the relaxation time t_0 (the time constant) is defined from the relation^{13,24)}

$$t_0 = \text{removed material} / \text{initial transport} = M / j_0 \quad (2.9)$$

where $j = V y_p(x_0) = L x_0 \alpha n$, $M = M_0 - M_p = \Omega_x^{\text{col}}(x_0 - x) + \Omega_y^{\text{col}}(y_0 - y)$; Ω , holdups.

More accurately $t_0 = (1 - \lambda)t_0$, the correction λ is estimated from the accurate solution²⁴⁾. As in case of any separating cascades the similarity of the stationary and non-stationary concentration distribution corresponds to eq. (2.8). The degree of approximation

x) Introduction of the coefficients of decontamination from Ru and Zr as separate factors is useful owing to the different effect of acidity, the scrubbing temperature, etc. on them.

xx) $\frac{\partial^2 x}{\partial z^2} + (n \frac{dy_p}{dx} - 1) \frac{\partial x}{\partial z} - (\tau_x + n \frac{dy_p}{dx} \tau_y) \frac{\partial x}{\partial t} + (\tau_x + \tau_y) \frac{\partial^2 x}{\partial z \partial t} - \tau_x \tau_y \frac{\partial^2 x}{\partial t^2} = 0$; $y_p = \alpha x$; $\bar{z} = z/h$
 $\bar{z} = z/\text{HTU}$; $\bar{H} = N$; τ , HTU time (= HTU holdup/flow); x, y , averaged x, y .
 e.g. $\bar{x} = \int_0^1 x dz / H \approx x_0 / \varepsilon N$; $x_p = x_0 [(1 + \varepsilon) e^{-(N-2)} - 1] / [(1 + \varepsilon) e^{\varepsilon N} - 1] \approx x_0 e^{\varepsilon \bar{z}}$; $\varepsilon = \alpha n \cdot 1$.

to equilibrium $\psi = (x_0 - x)/(x_0 - x_p) = 1 - e^{-t/t_0}$ depends on time rather than on the coordinate. Time of equilibrium setting in is $(3-5)t_0$, which corresponds to $\psi = 0.95-0.99$. The starting period curve found experimentally for the column of $\phi 200\text{mm}$, $H=2.8\text{m}$, with Rashig's rings of $25 \times 25 \times 4.5\text{mm}$ ($x_U^0 = 35\text{g/l}$, $x_H^0 = 0.5\text{m/l}$, $n=V/L=1$, $\alpha=1$) is close to the exponent (fig. 9a) while the relaxation time is close to that calculated from eq. (2.9).

| L=230 l/hr; $\tau_{\text{column}}=14,6\text{min}$ | | | | L=300l/hr, $\tau_{\text{column}}=11,2\text{min}$ | | |
|---|------|------|-------|--|-------|-------|
| Pulsation intensity, J=af, mm/min | | | | | | |
| | 0 | 4x78 | 4x108 | 0 | 4x54 | 4x108 |
| HETS, m | 1.11 | 0.95 | 0.65 | 1.11 | 0.905 | 0.565 |
| t _o , min, calc. | 4.35 | 4.8 | 5.6 | 3.3 | 3.7 | 4.35 |
| t _o , min, exp. | 3.3 | 4.8 | 5.6 | 2.6 | 3.2 | 4 |

When starting from a blank solution the expression for the x_{outlet} is close to the exponent (2.8) ($t_0 = M/j_0$, $M = \int_0^L x \cdot \bar{X} + \int_0^L y \cdot \bar{Y}$; $j_0 = Lx_0$) with delay. In case of nonlinear extraction isotherms (uranyl nitrate in wide ranges of concentrations and acidities) the process equations were solved with the help of E.C. Simultaneously the dynamic characteristics of the pulsed column of $\phi 200\text{mm}$, 4.2m high with a packing of $15 \times 15 \times 1\text{mm}$ were experimentally determined while starting up from a "solution" ($x_U^0 = 250\text{g/l}$, $x_H^0 = 1.55\text{m/l}$, $y_{N+1}^0 = y_U^0 = 0.2\text{g/l}$, $T_0 = 0.8\text{m/l}$, $L = 75\text{ l/hr}$, $V = 315\text{ l/hr}$) and from an acid ($x_U^0 = 0$, $x_H^0 = 2\text{m/l}$) with $L = 700\text{ mm/min}$. The starting period curves for uranyl nitrate are close to the exponents (fig. 9c, f) with the lag time $\Delta \tau$ which increases with moving away from the bottom of the column (it being the disturbance source, i.e. not saturated Q.p.). By contrast, in starting up from an "acid" when the concentration front moves down the column the time $\Delta \tau = z/w_c$ is increased from the top to the bottom (fig. 9e, f). $M_p \approx 19\text{kg}$ is removed, $j_0 = 27\text{kg/hr}$ and eq 2.9 gives $t_0 = 0.7\text{hr} > t_0^{\text{exp}} \approx 0.4\text{hr}$. When starting up from an acid $M_p = 7\text{kg}$, $j_0 = 17.5$ and $t_0^{\text{calc}} = 0.4\text{hr}$ ($t_0^{\text{exp}} \approx 0.3\text{hr}$).

The results of the transition process computations are close to the experimental data

Masstransfer

The Driving force (D.f.) With non-linear extraction isotherms the boundary concentrations x_1 and $y_1 = \alpha_1 x_1$ cannot be excluded by a simple procedure from the expressions for the flux through the x) $\int_{x_i} dx_i/dt + \int_{y_i} dy_i/dt = L(x_{i-1} - x_i) + V(y_{i+1} - y_i)$; \int_{x_i} , i -stage holdup.

diffusion Boundary layers^{x)}, the standard masstransfer equation becomes incorrect. In case of the nonelectrolyte distribution the task may be solved using the irreversible process thermodynamics according to which the diffusion flux is proportional to the chemical potential gradient: $j = -D_0 c d\mu/dz = \tilde{B}(a - a_1)$, where $\tilde{B} = D_0 RT / \delta = (B/\delta)$ (averaged). $da/dz \approx (a - a_1)/\delta$. With the equilibrium condition $a_y = K a_x$ one obtains the general masstransfer equation with the D.f. expressed in terms of the activities: $j = A_y(a_y^* - a_y) = A_x(a_x - a_x^*)$; $1/A_y = 1/\tilde{B}_y + K/\tilde{B}_x$; $a_y^* = K a_x$; $A_x = K A_y$. An alternative useful method for the electrolyte extraction (when it is difficult to average B) is the calculation of the boundary concentrations. Let $y_p = F(x)$ and $x - x_1 = \Delta X$, then $y_1 = F(x_1) = F(x - \Delta X)$ and the flux is $j = B_x \Delta x = B_y F(x - \Delta x) - y$. Knowing F and B one can obtain $\Delta X, x_1, y_1$ and j (or directly j , substituting ΔX by j/B_x) from this equation. It is possible, e.g. to expand $F(x - \Delta X)$ in a series on $\Delta x = j/B_x$ power. It gives $j = K_y(y_p - y)$, $1/K_y = 1/B_y + (y_p' + \Delta)/B_x$. The correction $\Delta \approx n(y_p - y)/(y_p' + B_x/B_y)^{xx}$ depends on B_y , therefore with $(y_p - y)$ D.f. the resistances are not quite additive.

Masstransfer in a real apparatus is complicated by longitudinal diffusion, axial mixing (am) by the macroflows, and by transverse non-uniformity (tn). All these effects may be approximately described by a longitudinal diffusion with the effective coefficient $D_{ef} = D_T + D_{am} + D_{tn}$ resulting in the HTU increase;

$$h = h_k + D_{ef} x / w_x + D_{ef} y / w_y = h_k + h_{D,x} + h_{D,y} \quad (3.13)$$

where h_k is HTU defined by the masstransfer coefficient; w the velocity $h_k = w/kS$, $h_D = h_T + h_{am} + h_{tn}$; $h_T = D_x/w_x$, $h_{tn} = D_{tn} x / w_x + D_{tn} y / w_y$.

The transverse non-uniformity (inconsistency of the flow rates over the column cross-section) is of a particular importance as it is the principal reason of apparatus effectiveness lowering with a diameter and height increase (h may be 5 and more times higher than h_k). The diffusion correction $h_D = D/w$ is large with low rates, therefore the effectiveness of columns of a large diameter increases with the flow rates (fig. 11a, $h_{tn} = h - h_k$; h_k = HETS of column 25mm in dia. If D_y is decreased with the increase of the hole numbers and D_x drops with sectioning and in the latter case $D_y = D_x = 1.5 \text{ m}^2/\text{hr}$, then curve 1 cores-

x) $j = B_x(x - x_1) = B_y(y_i - y)$, where $B = D/\delta$, the masstransfer coefficient; δ , diffusion boundary layer thickness²⁾, hence $j = \tilde{K}(\alpha_i x - y)$; $1/\tilde{K} = 1/B_y + \alpha_i/B_x$; D.f. is $(\alpha_i x - y) > (y_p - y)$,

xx) more accurately $\Delta = -(j/B_x) y_p''/2! + (j/B_x)^2 y_p'''/3! - \dots$ where $y_p^{(n)} = d^n F(x)/dx^n$

xxx) more accurately $h_{oy} = h_k + h_{Dx} [1 + (\alpha n - 1) h_k/h] + h_{Dy} [1 + (\alpha n - 1) h_{Dx}/h] / [1 - (\alpha n - 1) h_{Dy}/h]$

346

ponds to $D_y = 5.5 \text{ m}^2/\text{hr}$, $D_x = 3.5$, the o.p.t.n. is greater than i.n. a.p.). The pattern peculiarity is an anisotropy, a large difference in the diffusion coefficients in the longitudinal (D_{ef}) and transverse ($D_{\perp} = D_T + D_{am}$) directions: $D_{ef} = D_{\perp} + D_{tn} > D_{\perp}$. As the transverse non-uniformity decreases with the mixing intensification one may expect^{11b)} that $D_{th} = C_1/D_1^m$ (where D_{th} i.e. C_1 is increased with the column diameter, $C_1 \sim d_{col}^2$ or $\exp d_c$) and $D_{ef} = D_{\perp} + C_1/D_1^m$ ¹¹⁾ so that 1) D_{ef} and D_{\perp} should come nearer when turbulentized. (This assumption is confirmed by fig. 11c). 2) Opposite to the small columns, in large dia columns the pulsation may lower D_{ef} due to the transverse non-uniformity decrease ($D_{tn} = C_1/(D_0 + C_2 d_{pack} J)^m$ and C_1 is high). In fact, for 500mm dia column at $W = 7 \text{ m/h}$ without pulsation $D_x = 2 \text{ m}^2/\text{h}$, with $I = 500 \text{ mm/min}$ $D_x = 1 \text{ m}^2/\text{h}$, for 100mm column $D_x = 0.5$ and $0.85 \text{ m}^2/\text{h}$, resp. (as $D_T = D_T^0 + C I d_p$). It is important that the transverse non-uniformity is a hydraulic phenomenon therefore its study and elimination is possible using hydraulic scale-up without the experiments with mass transfer^{x)}. Constructive measures result from the theory based on the channeling pattern²⁴⁾:

$$h_{tn} = l_x (\Delta L_x / L_x) + l_y \Delta L_y / L_y$$

where $\Delta L/L$ is the flow fraction evading the mass transfer, l is the by-pass length. These measures consist in the diminishing of L by setting phase distributors and the decrease of l by the apparatus sectioning, providing for the transverse flow mixing; a good mixing is obtained by means of "louver" rotary plates²⁸⁾.

The distribution of the dispersed phase in the packed column 700mm in diameter was studied by hydraulic scale-up. With the pulsation intensity increase the feed cone section expands while the number of feed sources required for the uniform distribution is decreased (fig. 12b). Flow density levelling off with pulsation was also observed for the distributors of a hydraulic seal type (fig. 12c, d). The uniformity degree of the continuous phase motion may be controlled by an impulse method^{13b)}; it being important to scale up the density gradient that increases the by-pass length and, correspondingly, HETS in the uranium zone (fig. 5c, also²⁸⁾).

Mechanism of the extraction intensification is often associated with the surface renewal, i.e. with the increase of the mass transfer

x) Thus, the effectiveness of 5m in dia distillation plates with a directed motion was increased by 50%²⁴⁾.

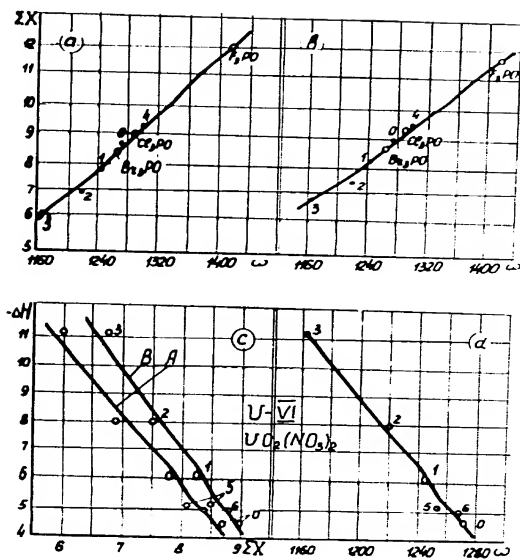
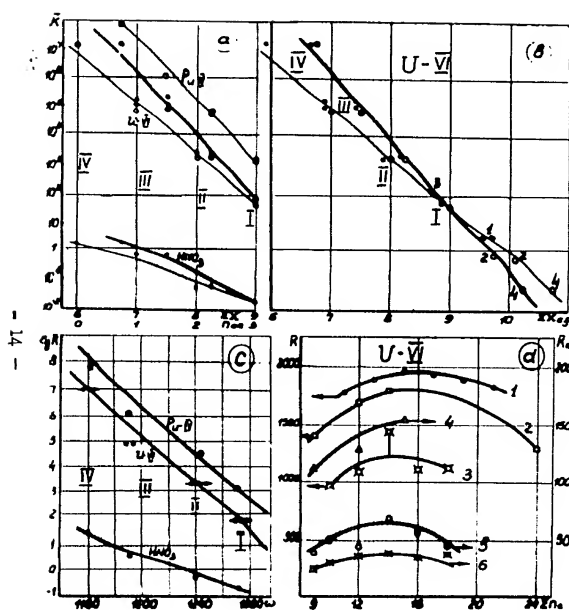
coefficient. The analysis of the elemental components of the process and of the experimental data on the sieve-plate and packed pulse columns¹¹⁾ showed that the effectiveness rise is due to the increase of the phase contact surface, while the effective coefficient of mass-transfer is even decreased, $K_m < 1$, fig. 15a. ($K_E = h_0/h$; $K_R = d_0/d$; $K_\Omega = \Omega/\Omega_0$, $K_S = S/S_0$ and $K_m = k/k_0$ are coefficients of effectivity, dispersion holdup surface and mass transfer variation index "o" denotes the value before intensification; $K_E = K_R K_m K_S$). In the first approximation the Ω and k variations are secondary and are defined by the drop diameter decrease^{x)}. Then the knowledge of the dependence 1) of the drop radius on the intensification variable (revolutions n , pulsation intensity I) and 2) of the terminal velocity and the mass transfer coefficient on the drop diameter d is sufficient to advance a quantitative theory. The dependences of d on the intensity of $I/d \sim V^{1-1.5}/G^{0.5}$ type found for various apparatuses^{11,12)} correspond to the theoretical ones²⁵⁾, i.e. the drop size is determined from the general regularities of a dispersion in a turbulent flow. The terminal drop velocity dependence u on its diameter is seen from fig. 14a (generalised coordinates, $Q = u/\sigma$, $R = d/\sqrt{g\Delta\rho/\sigma} \approx d/d_{max}$, $S = d\rho\sigma/\mu^2 \approx d/d_{min}$; $T = \rho\sigma^{3/2}/\mu^2\sqrt{g\Delta\rho} = S/R = d_{max}/d_{min} = \sqrt{P}$). The flooding flow rate w_f proportional to the terminal drop velocity should be decreased when dispersed; the dependence of w_f on I should reproduce fig. 14a in a mirror image which is really observed (fig. 15b,c), $w_f \approx w_f^0/[I + 0.265(cI_{ef})^2]$ ^{12) x)}.

The increase of hold-up with the intensity may be described by Pratt's eq. as the characteristic velocity ($v_0 \sim w_f \sim U$) depends on I ; hence, the dependences of Ω on I and on the flow rates are similar and are defined by the degree of approximation to the flooding conditions $\varphi = w/w_f$ ¹¹⁾. The mass transfer coefficient is somewhat decreased on dispersion which together with the longitudinal diffusion growth accounts for the dependence of K_m on I ¹¹⁾. The effectivity increase of packed-pulsed columns in two systems at $I < 2m/min$ is approximately described by the eq. $K_E = 1 + b_E I_{ef}^2$ ¹²⁾ (fig. 15d), where $b_E = 1.7$ (if $d_{col}/d_{pack} < 7$, then $b \approx 0.25 d_{col}/d_{pack}$). At very high I HTU rises due to the drop coalescence (surface decrease) and to the influence of axial mixing¹¹⁾. To choose the optimum conditions criterion $\phi = w/h$ should be used^{11,24)}.

x) In the packed pulsed columns the filling becomes close packed resulting in w_f decrease.

References

1. Розен А.М. Атомная энергия, 2, (1957) 445. жур. Неорг. Хим., 8, (1963), 1003.
2. Розен А.М., Хорхорина Л.П. Ж. неорг. хим. 2 (1957) 1956, РадиоХим. 4, (1962), 594.
3. Розен А.М., Моисеенко Э.И. а) Ж. неорг. хим. 4 (1959) 1209, б) Радиохимия 2 (1960) 274, в) сб. "Экстракция" в 2, Атомиздат, (1962).
4. Розен А.М. Физическая химия экстракционных равновесий. Доклад на конф. 1959г. Сб. "Экстракция" в. I (1962).
5. Розен А.М., Хорхорина Л.П., Юркин В.Г. ДАН СССР 153 (1963) №6.
6. Розен А.М., Николотова З.И. Ж. неорг. химия 8 (1964) №7.
7. Адамский Н.М., Карпачева С.М., Мельников И.М., Розен А.М. Радиохимия а) 2 (1960) 13 б) 2 (1960) 400.
8. Розен А.М., Решетько Ю.В., Радиохимия 6 (1964) №6.
9. Розен А.М. Атомная энергия 7 (1959) 277.
10. Розен А.М., Елатомцев Б.В. а) Радиохимия 6 (1964) №6, б) те же и Лапавок Л.И. Хим. маш. (1964) №5.
11. Розен А.М. а) Докл. высш. школы, сер. энергетика (1958) №3, 173, б) сб. "Экстракция" в 2 (1962)
12. Розен А.М., Васильев В.А., Горшкова Г.А., Беззубова А.И. а) доклад АН СССР 136 (1961) 1461; б) Сб. "Экстракция" в 2 (1962).
13. Розен А.М. а) ДАН СССР 107 (1956) 295, б) ДАН СССР 122 (1958) 671.
14. Пушленков М.Ф., Комаров Е.В., Шувалов О.Н. Радиохим. 2 (1960) 537.
15. Шувалов О.Н. Пушленков М.Ф. Радиохимия 3 (1961) 668, 5 (1963) 536.
16. Burger L. J. Phys. Chem. 62, (1958) 590.
17. Тимошев В.Г. и др. Радиохим. 2 (1960) 419, сб. "Экстракция" в. I
18. Goldenson J. et. al. J. Am. Chem. Soc. 76 (1954) 5158.
19. Бацанов С. Электроотрицательность элементов. Новосибирск, 1962.
20. Glueckauf E., McKay H. Trans. Faraday Soc. 47, (1951) 428.
21. Goldenson J. et. al. J. Am. Chem. Soc. 77 (1955) 4473.
22. Newton T., Cowen G., J. Phys. Chem. 64 (1960), 244.
23. Rudstam C., Acta Chem. Scand. 13 (1959) 1481.
24. Розен А.М. сб. "Тр. Всес. конф. по применению изотопов" АН СССР 1958, теория разделения изотопов в колоннах. Атомиздат 1962г.
25. Левич В.Г. Физико-химическая гидродинамика, изд. АН СССР (1952).
26. Карпачева С.М., Медведев С.Ф. и др. Хим. маш. (1959), №3, (1963), No. 2
27. Аэров М.Э., Каган С.З., Волкова Т.С. Ж. прикл. хим. 36 (1963) 1994
28. Woodfield F., Sege G. Chem. Eng. Progr., Symp. ser. 50 (1964), 13.
29. Hu S, Kintner R. C. Am. Inst. Chem. Eng. J. 1, (1955), 42.



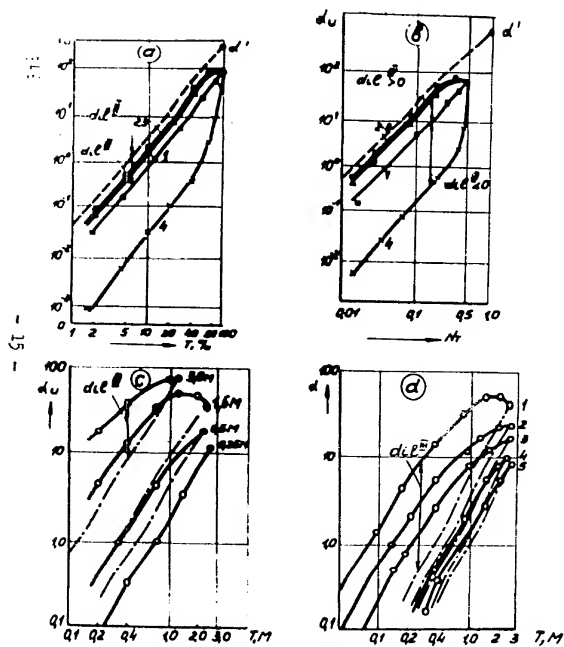


Fig. 3 Effect of diluents and HNO_3 on the extraction of metals by TBP.
(a, b) extraction of microamounts of uranyl nitrate from 2N HNO_3 .
Diluents: 1- CO_2 ; 2-benzene; 3-benzene; 4- CHCl_3 ; distribution coefficient in dry TBP; --- ideal solution.
(c, d) Extraction from nitric acid solutions. Diluent: benzene (data by Bleskina L.A.); 1-U(VI); 2-Np(VI); 3-Pu(IV); 4-Np(IV); 5-Th(IV) ($I_{\text{H}}=1.5\text{p}$); --- quasi-ideal solution.

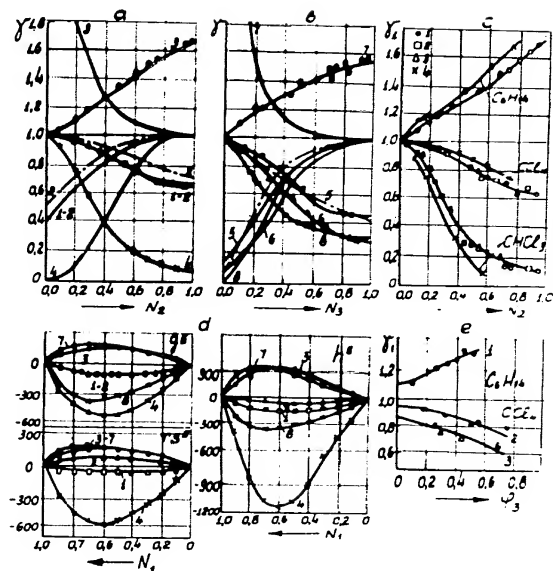


Fig. 4 Characteristics of the interaction of diluents with extractant and uranyl nitrate solvate.
Activity coefficients in the system diluent-TBP (a) and diluent-solvate (b); indexed lines (o, A, U, X) - γ_i , without indexes - γ_i or γ_i^* ; --- γ_i of athermal solution. Nos of curves correspond to the Nos of systems in table 11; (d) thermodynamic excess functions of the systems; (e) effect of substituting R groups by NO ones; o-TBP; A-DBBP; X-TBPO; (e) description of ternary system according to the characteristics of binary ones; / --- calculated.

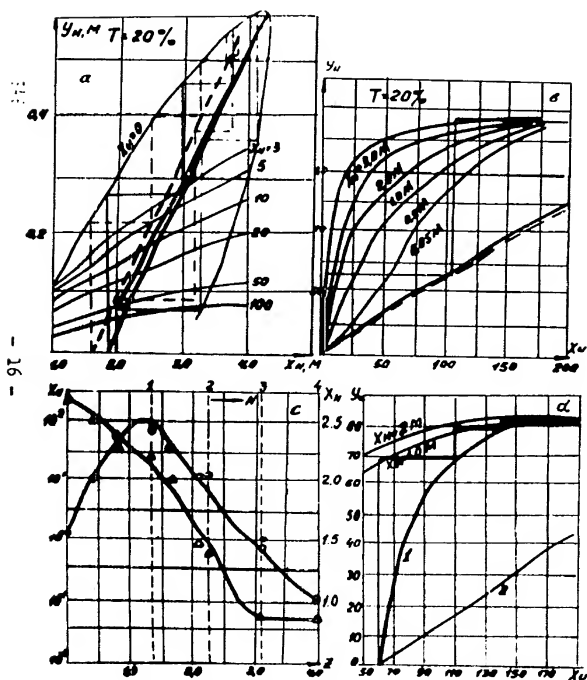


Fig. 5 Calculation of the macrocomponent distribution over the extractor stages.
(a) KNO_3 ; (b) uranyl nitrate, $\alpha/1$ (— calculation with the volume changes being neglected); (c) distribution of uranyl nitrate and acid over the column height (a and c—experimental; a and c—calculated); (d) operating line of nonstationary (1) and stationary (2) processes.

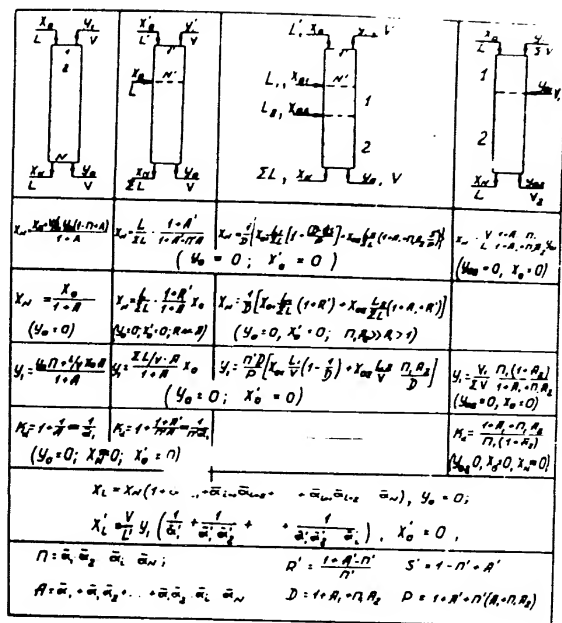


Fig. 6 Calculation of the distribution of elements present in microamounts for the extractors with various flow sheets.
 α —distribution coefficient over the 1-stage; $\tilde{\alpha}_L$ — α extraction factor; K —nos of stages; A —cascade extraction factor; R —recirculation coefficient when scrubbing; K —decontamination factor.

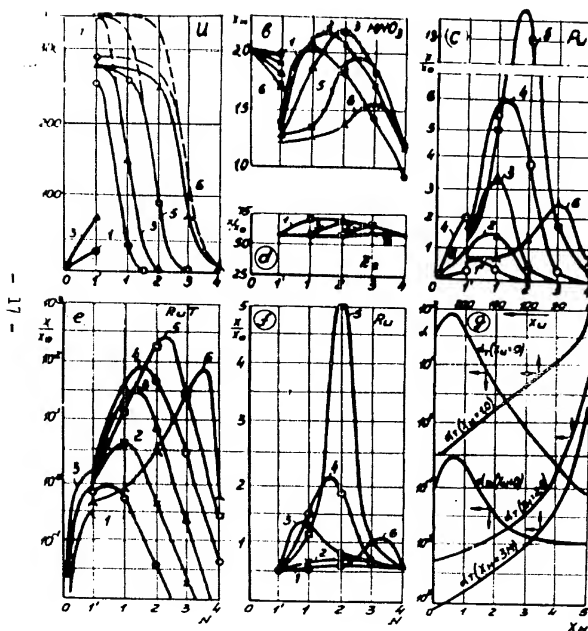


Fig.7 Effect of degree of approximation to the limiting conditions on the distribution of compounds over the extractor stages.
(a) $U, g/l$; (b) $Pu, g/l$; (c) Zr ; (d) Ru ; (e, f) Ru and Ru (without disproportionation); values of η : 1-0.76; 2-0.90; 3-0.99; 4-0.99; 5-0.9999; 6-0.999999; 7-0.9999999; (g) distribution coefficients of Ru and $RuD(X_{U, g/l}; X_{H, m/l})$.

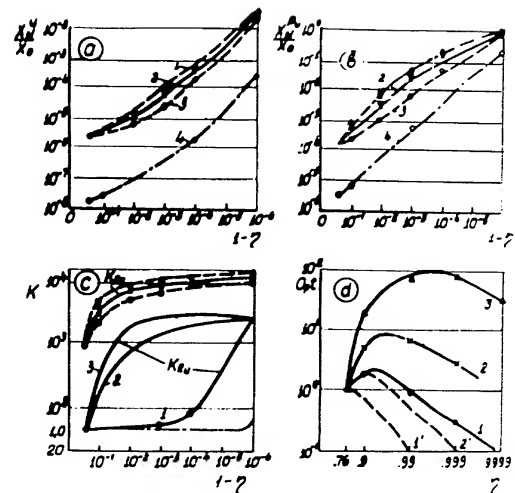


Fig.8 Static characteristics of the extractor and their optimization.
Waste $U, g/l$, (a) and $Pu, g/l$, (b) concentrations vs η ; 1, 2, 3 - variations of T or V, L_0 and $X_{U, g/l}$ respectively; 4 - curve 2 with one additional extraction stage; (c) factor of decontamination from Zr and Ru . 1 - reaction $RuB-RuD$ does not proceed; 2 - reaction is rapid; 3 - RuB is not accumulated; - - - - - curve 1 at $N=6$; (d) optimization criterion vs η (1, 2' - curves 1, 2 without the RuB disproportionation).

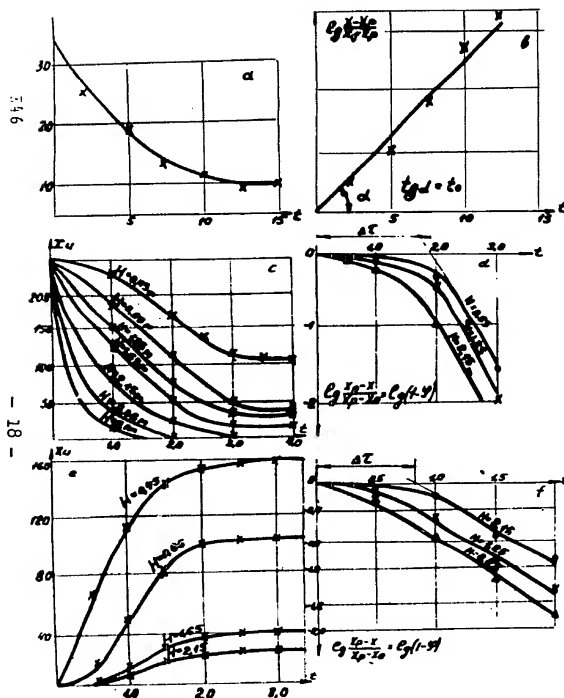


Fig. 9 Dynamics of the pulsed column of 200mm (starting period curves for uranyl nitrates in different column sections). Starting from operating (a,b,e,d) and blank (e,f) solutions; (a,b) system with $\omega=1$ at $I=42\text{mm/min}$ $X_{u,0}/l$; t, hr; N, m.

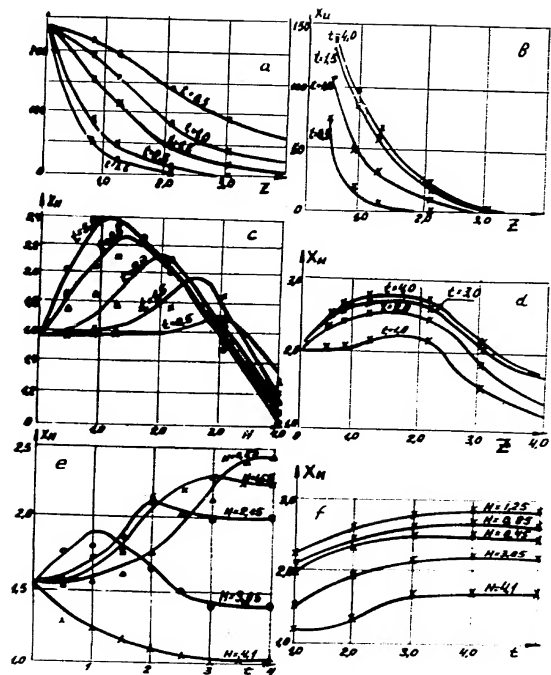


Fig. 10 Transition processes in the extraction column. Distribution of the concentration of uranyl nitrate (a,b) and HNO_3 (c,d) over the column height when starting from initial (a,c) or blank (b,d) solutions. Starting period curves for nitric acid when starting from initial (e) and blank (f) solutions; $X_{u,0}/l$; $X_{H,0}$; t, hr; N, m.

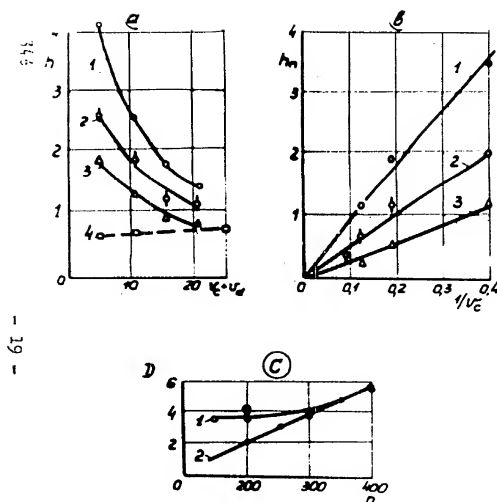


Fig. 11 Characteristics of transverse nonuniformity of the extractor.

(a) Load characteristics of the packed column of 400mm (I - a distributor with 50 holes; II - with 200 holes; 3 - sectioning) and of 25mm (curve 4) in case of uranyl nitrate extraction^{28,14b};
 h, HETS, $\mu\text{m/hr}$;
 (b) applicability of the diffusion pattern;
 (c) $D_{eff}(1)$ and $D_{eff}(2)$, cm^2/sec vs revolutions n, min^{-1} of the column of 400mm²⁷.

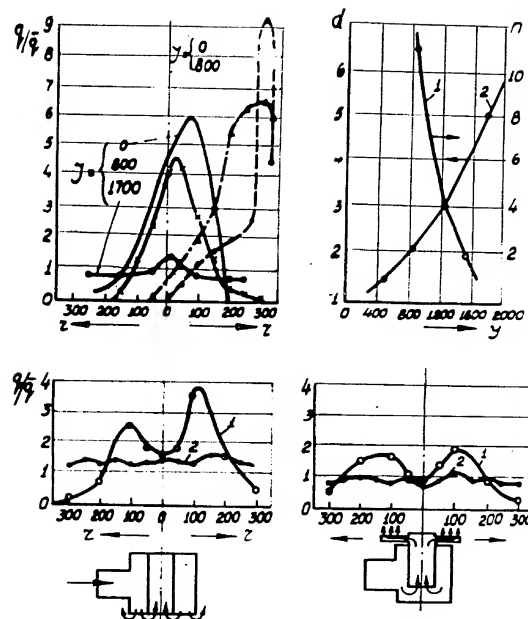


Fig. 12 Hydraulic scaling up of dispersed phase distribution in the extraction column.

(a) Relative dispersed phase distribution density q/q_0 (single feed source in the centre and near the wall of column; r, mm ; I_p, min); (b) effect of pulsation intensity I_p, min , on the necessary feed source number (1) and the feed cone diameter, $d_{cm}(2)$; (c) dispersed phase distribution over the column cross-section, 1. $I=0$, 2. $I=1500$.

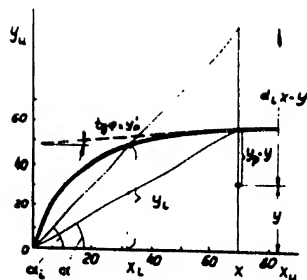


Fig. 13 Mass transfer in case of nonlinear extraction isotherms.

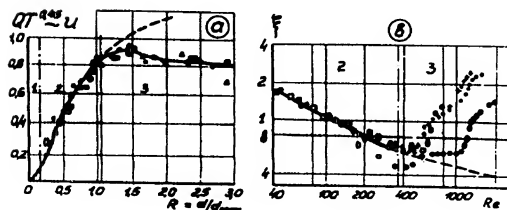


Fig. 14 Hydrodynamics of drops.

(a) Terminal velocity u of a drop vs its diameter (generalized coordinates, calculated from data [20]). Systems: water-tetra-bromethane; α -dibromethane, α -ethyl-bromide; α -bromobenzene, n -nitrobenzene, n -nitrotoluene, α -chlorobenzene. (b) Drag coefficient vs Reynolds number; --- rigid spheres.

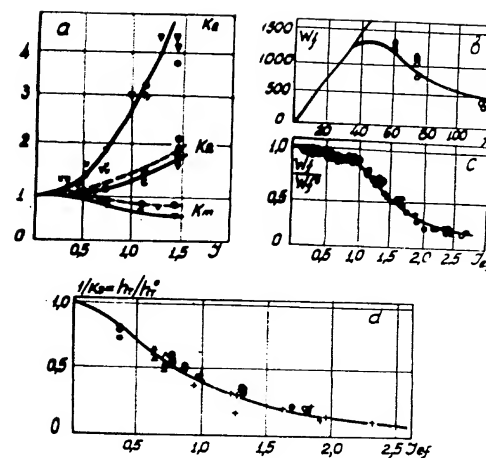


Fig. 15 Effect of the pulsation intensity I on the extractor characteristics.

K_L , K_R and K_M (a) (column of $\phi 100$ mm). The limiting loads of sieve plate (b) and packed (c) columns. (d) HETS; \circ , Δ , $+$ - columns 100, 200 and 400 mm in diameter, respectively; packing of $15 \times 15 \times 0.6$ mm [2, 26]; --- correlation [2] $I_{ef} = 1.5 \cdot 10^3 \cdot c(f=100)$, m/min; $I = af$.

Fig.1 Effect of structure on the extraction power of neutral organophosphoric compounds.

(a,c) effect of substituting R groups by RO ones; (b) total correlation; I $(RO)_3PO$; II $(RO)_2RPO$; III ROR_2PO ; IV R_3PO ; 1 $(RO)_2PhPO$; 2 $(C_2H_4Cl)_3PO$; 3 $(RO)_2PhPO$; 4 $(RO)_2CCl_3PO$; ●-our data; ○-calculated from data¹⁶; ---scale¹⁸; —scale(1,3); (d) effect of the length of the hydrocarbon chain, calculated from the data: 1-⁶; 2,4-¹⁶; (phosphonates); 5,6-¹⁶ (phosphates).

Fig.2 Electronegativity and its effect on the extraction.

(a) scale(1.2), $X_F=4$; $X_{Cl}=3.0$; $X_{Br}=2.8$; (b) scale(1.3); $X_F=3.9$; $X_{Cl}=3.1$; $X_{Br}=2.9$; (c)(d) dependence of the binding energy ($\approx -\Delta H$ kcal/mole) on ΣX and ω_{PO} , cm^{-1} , A, B -scale(1.2)(1.3); 0-TBP; TOP; 1-methylphosphates; 2-ODOP; 3-TOPO; 4- $(PhO)_3PO$; 5-dihexylphenylphosphonate; 6-dihexylchloromethylphosphonate.

Fig.3 Effect of diluents and HNO_3 on the extraction of metals by TBP.

(a,b) extraction of microamounts of uranyl nitrate from 2M $NaNO_3$.
Diluents: 1- CCl_4 ; 2-kerosene; 3-benzene; 4- $CHCl_3$; α' -distribution coefficient in dry TBP; --- ideal solution.
(c,d) Extraction from nitric acid solutions. Diluent: benzene (data by Bleskina L.A.): 1-VI; 2-Np(VI); 3-Pu(IV); 4-Np(IV); 5-Th(IV) ($X_H=1,5M$); --- quasi-ideal solution.

Fig.4 Characteristics of the interaction of diluents with extractant and uranyl nitrate solvate.

Activity coefficients in the systems diluent-TBP(a) and diluent-solvate (b); indexed lines (O, Δ , \square , \times) - γ_1 , without indexes - γ_2 or γ_3 ; - - - γ of athermal solution. Nos of curves: 1,5 CCl_4 diluent; 2,6 C_6H_6 ; 3,7 hexane, 4,8 $CHCl_3$; (d) thermodynamic excess functions of the systems; (c) effect of substituting R groups by RO ones; ○-TBP; \square -DBBP; Δ -BDBP; X-TBP; (e) description of ternary systems according to the characteristics of binary ones; / — calculated/.

346

Fig.5 Calculation of the macrocomponent distribution over the extractor stages.

(a) HNO_3 ; (b) uranyl nitrate, g/l (--- calculation with the volume changes being neglected); (c) distribution of uranyl nitrate and acid over the column height (Δ and o-experimental; \blacktriangle and \bullet -calculated); (d) operating line of nonstationary (1) and stationary (2) processes.

Fig.6 Calculation of the distribution of elements present in microamounts for the extractors with various flow sheets.

α_1 - distribution coefficient over the 1-stage; $\bar{\alpha}_1 = \alpha_1 n$ extraction factor, N-Nos of stages; A-cascade extraction factor; R- recirculation coefficient when scrubbing; K-decontamination factor.

Fig.7 Effects of degree of approximation to the limiting conditions on the distribution of compounds over the extractor stages.

(a) U, g/l; (b) HNO_3 , m/l; (c) Pu; (d) Zr; (e,f) RuT and Ru (without disproportionation; values of η : 1-0,76; 2-0,90; 3-0,99; 4-0,99; 5-0.9999; 6-0.999999; N-Nos of stages; (g) distribution coefficients of RuT and RuD (X_U , g/l; X_H , m/l).

Fig.8 Static characteristics of the extractor and their optimization.

Waste U, g/l, (a) and Pu (b) concentrations vs η ; 1, 2, 3, -variations of T or V, L_0 and X_U^0 respectively; 4 - curve 2 with one additional extraction stage; (c) factor of decontamination from Zr and Ru.

1-reaction RuT \rightarrow RuD does not proceed; 2-reaction is rapid; 3-RuT is not accumulated; --- curve 1 at N=6; (d) optimization criterion vs η (1, 2' -curves 1.2 without the RuT disproportionation).

346

- 22 -

Fig.9 Dynamics of the pulsed column of ϕ 200mm
(starting period curves for uranyl nitrates
in different column sections).
Starting from operating (a,b,c,d) and blank (e,f) solutions;
(a,b) system with $\alpha = n=1$ at $I=4 \times 78 \text{ mm/min}$, $X_U, \text{g/l}$; t, hr ; H, m .

Fig.10 Transition processes in the extraction column.
Distribution of the concentration of uranyl nitrate (a,b) and
 HNO_3 (c,d) over the column height when starting from initial
(a,c) or blank (b,d) solutions. Starting period curves for
nitric acid when starting from initial (e) and blank (f) solu-
tions; $X_U, \text{g/l}$; X_H, M ; t, hr ; H, m .

Fig.11 Characteristics of transverse nonuniformity
of the extractor.
(a) Load characteristics of the packed column of $\phi 400 \text{ mm}$
(I- a distributor with 50 hole; II-with 200 holes; 3-section-
ing) and of $\phi 25 \text{ mm}$ (curve 4) in case of uranyl nitrate extrac-
tion^{26, 11b}; $h, \text{HETS, m}$; $V, \text{m/hr}$;
(b) applicability of the diffusion pattern;
(c) $D_{ef}(1)$ and $D_T(2)$, cm^2/sec vs revolutions $n \text{ min}^{-1}$ of the
column of $\phi 200 \text{ mm}$ ⁵⁰.

Fig.12 Hydraulic scaling up of dispersed phase
distribution in the extraction column.
(a) Relative dispersed phase distribution density q/\bar{q} (single
feed source in the centre and near the wall of column; r, mm ;
 $I, \text{mm/min}$); (b) effect of pulsation intensity $I, \text{mm/min}$, on the
necessary feed source number (1) and the feed cone diameter,
 $d_{cm}(2)$; (c) dispersed phase distribution over the column
cross-section, 1. $I=0$; 2. $I=1500$.

Fig.13 Mass transfer in case of nonlinear extraction
isotherms.

Fig.14 Hydrodynamics of drops.

(a) Terminal velocity u of a drops vs its diameter (generalized coordinates, calculated from data²⁹). Systems: water+
 Δ - tetrabromethane; \blacksquare - dibromethane, \square - ethyl-bromide;
 \bullet - brombenzene, o - nitrobenzene, $+$ nitrotolylene, \blacktriangle - chlor-
 benzene. (b) Drag coefficient vs Reynolds number; --- rigid
 spheres.

Fig.15 Effect of the pulsation intensity I on the
extractor characteristics.

K_R, K_{Ω} and K_m (a) (column of ϕ 100mm). The limiting loads of
 sieve plate (b) and packed (c) columns.
 (d) HETS; $o, \Delta, +$ - columns 100, 200 and 400mm in diameter,
 respectively; packing of $15 \times 15 \times 0.6$ mm^{12, 26}; --- correlation¹²
 $I_{ef} = I_e^{c(f-100)}$, m/min; $I = af$.